



A turn-on chemosensor based on naphthol–triazole for Al(III) and its application in bioimaging

Tian-Jing Jia, Wei Cao, Xiang-Jun Zheng*, Lin-Pei Jin

Beijing Key Laboratory of Energy Conversion and Storage Materials, College of Chemistry, Beijing Normal University, Beijing 100875, PR China

ARTICLE INFO

Article history:

Received 13 February 2013

Revised 17 April 2013

Accepted 26 April 2013

Available online 3 May 2013

Keywords:

Al(III) sensor

Schiff base

Fluorescence

Turn-on

Cell imaging

ABSTRACT

A new Schiff base 1-[(1H-1,2,4-triazole-3-ylimino)-methyl]-naphthalene-2-ol (H_2L) exhibiting high selectivity for Al^{3+} ion over other metal ions, such as Li^+ , Na^+ , K^+ , Ca^{2+} , Mg^{2+} , Cu^{2+} , Co^{2+} , Mn^{2+} , Ni^{2+} , Zn^{2+} , Cd^{2+} , Pb^{2+} , Fe^{3+} , and Cr^{3+} was prepared, and it is sensitive for Al^{3+} with the detection limit reaching $0.69 \mu M$ in DMF. Upon addition of Al^{3+} , the significant enhancement (32-fold) of fluorescence intensity for H_2L at 466 nm is ascribed to the formation of a 1:1 complex between Al^{3+} and H_2L , which is denoted as the chelation-enhanced fluorescence (CHEF) effect. The confocal fluorescence microscopy experiments demonstrate that H_2L could be used as a fluorescent probe for Al^{3+} in living cells.

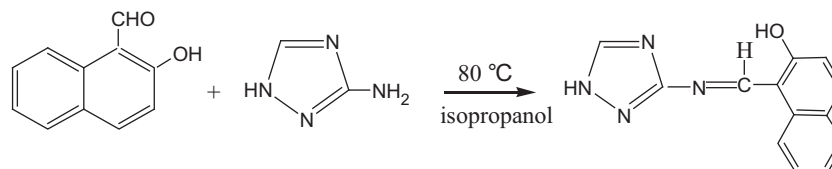
© 2013 Elsevier Ltd. All rights reserved.

Aluminum is the third most prevalent element and the most abundant metal in the biosphere, accounting for approximately 8% of the Earth's mass, and extensively used in modern life.¹ Aluminum in its ionic form (Al^{3+}) is found in most animal and plant tissues, and in natural waters. High concentration of Al^{3+} hampers plant performance,² killing fish, algae, bacteria, and other species in aquatic ecosystems.³ Also, Al^{3+} causes neurofibrillary, enzymatic, and neurotransmitter changes in the central nervous system. Human illnesses such as dementia and encephalopathy, Parkinson and Alzheimer diseases are believed to be attributed to the toxicity of Al^{3+} .^{4,5} Therefore, the facile detection of Al^{3+} is crucial in environmental monitoring and biological assays, and remains a major requirement. However, compared to other transition metal ions, limited examples of fluorescence sensors based on small molecules for Al^{3+} have been reported.^{6,7}

Nitrogen and oxygen-rich coordination environments can provide a hard-base environment for the hard-acid Al^{3+} . Moreover,

the nitrogen and oxygen donor sites can contribute to the high stability of the resultant complexes.⁸ Thus, we selected 2-hydroxy-1-naphthaldehyde as a fluorophore and binding moiety, and 3-amino-1H-1,2,4-triazole as a synergic ligand to provide more coordination sites for metal ions to synthesize a new Schiff base, named as 1-[(1H-1,2,4-triazole-3-ylimino)-methyl]-naphthalene-2-ol (H_2L).

H_2L was synthesized as shown in Scheme 1 and characterized by elemental analysis, IR, and single-crystal X-ray diffraction (see Supplementary data). The crystallographic data and structure refinement, and key bond distances and bond angles of H_2L are listed in Tables S1 and S2. The crystal structure of H_2L is shown in Figure 1. The bond distance of C3–N4 is 1.292 Å, indicating the feature of a double bond. The double bond, $-C=N-$ links the triazole and naphthalene moieties to a coplanar molecule. Single crystal X-ray diffraction reveals that intramolecular and intermolecular hydrogen bonds exist in H_2L . The O–H...N (1.817 Å) intramolecular



Scheme 1. The synthesis of H_2L (2-hydroxy-1-naphthaldehyde, 3-amino-1H-1,2,4-triazole, isopropanol, 80 °C, yield: 57%).

* Corresponding author. Tel.: +86 1058805522.

E-mail address: xjzheng@bnu.edu.cn (X.-J. Zheng).

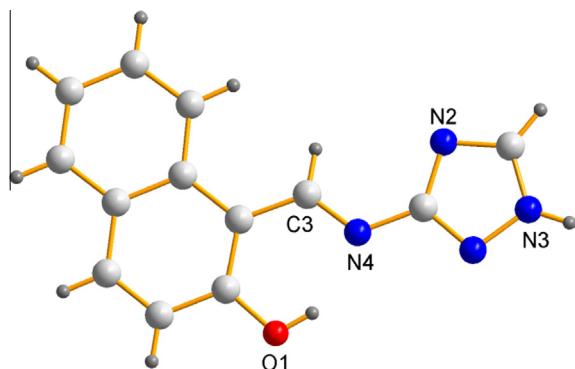


Figure 1. The crystal structure of chemosensor H₂L.

hydrogen bonds are formed between the oxygen atom (O1) of naphthol hydroxyl and the nitrogen atom (N4), and the N–H...N (2.191 Å) intermolecular hydrogen bonds are formed between the nitrogen atom (N2) of triazole moiety and nitrogen atom (N3) from another molecule.

The excitation and emission spectra of H₂L are shown in Figure S1. When H₂L is excited at 288 nm, a broad emission band can be observed at 348 nm, while H₂L shows weak emission upon excitation at 442 nm. However, upon addition of Al(NO₃)₃, the fluorescence intensity of H₂L increased by a factor of 32 at 466 nm when excited at 442 nm owing to the formation of a complex between H₂L and Al³⁺. In contrast, addition of other relevant metal ions, such as Li⁺, Na⁺, K⁺, Ca²⁺, Mg²⁺, Cu²⁺, Co²⁺, Mn²⁺, Ni²⁺, Zn²⁺, Cd²⁺, Pb²⁺, Fe³⁺, and Cr³⁺ has almost no fluorescence enhancement. The fluorescence response behavior of H₂L upon addition of various metal ions in DMF is shown in Figure 2a. The selectivity of H₂L to Al³⁺ was plotted as a bar graph in Figure 2b; only Al³⁺ resulted in a pronounced fluorescence enhancement relative to the control ions. To evaluate the selectivity of H₂L to Al³⁺ in practice, the systems of Al³⁺ coexisting with other metal ions were examined in DMF. As shown in Figure 2c, relatively low fluorescence intensities were observed in the presence of other metal ions except Pb²⁺. The response of H₂L for Al³⁺ in the presence of Fe³⁺ was obviously low but can be detectable. There was almost no fluorescence of H₂L upon addition of Pb²⁺ alone, however, the remarkable enhancement in fluorescence intensity of H₂L with Al³⁺ in the presence of Pb²⁺ ion was observed and should be attributed to a cooperative interaction which was triggered by Pb²⁺ ion.⁹ Pb²⁺ ion can combine with nitrogen atom of the triazole group, as well as the oxygen atom from naphthol hydroxyl, which may lead to fluorescence enhancement. When H₂L was titrated with Al³⁺, the fluorescence intensity increased steeply up to 7 equiv and then remained almost the same at the concentration over 13 equiv (Fig. 3). This could be attributed to the triazole group in H₂L to provide nitrogen atoms and more Al³⁺ ions are coordinated with them. Therefore, H₂L provided a wide sensing range for Al³⁺.

¹H NMR for H₂L is shown in Figure 4a. The assignment for H₂L was also confirmed by ¹H MBC, ¹H SQC, and H–H COSY (Figs. S2–S4). The binding mode of Al³⁺ with H₂L was examined by ¹H NMR spectra of H₂L in DMF-*d*₇ recorded upon addition of various amounts of Al³⁺ (Fig. 4). The proton signal of the naphthol hydroxyl at 14.37 ppm disappeared when Al³⁺ and H₂L were mixed in a 1:1 ratio (Fig. 4b), and at the same time, the proton signal of C=N was downfield shifted by 0.71 ppm. Furthermore, compared to ¹H NMR spectrum of H₂L upon addition of 1.0 equiv Al³⁺, ¹H NMR remained nearly unchanged upon addition of 1.5 equiv Al³⁺ (Fig. 4c). These results indicated that the nitrogen atom of imine and oxygen atom of naphthol hydroxyl were the binding sites for Al³⁺.

We then studied the absorbance changes of H₂L upon addition of metal ions (Fig. S5). The electronic absorption spectrum of H₂L

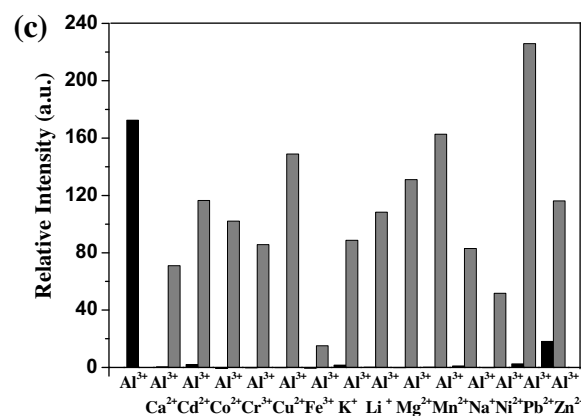
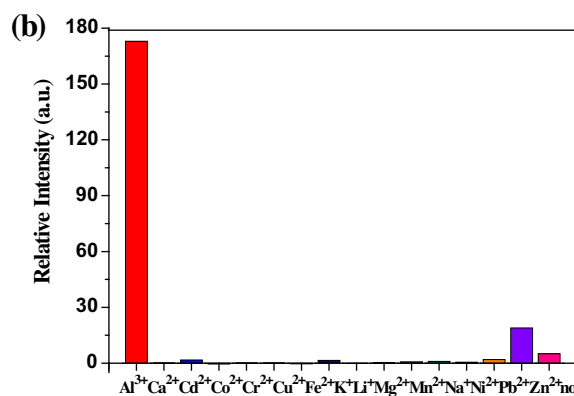
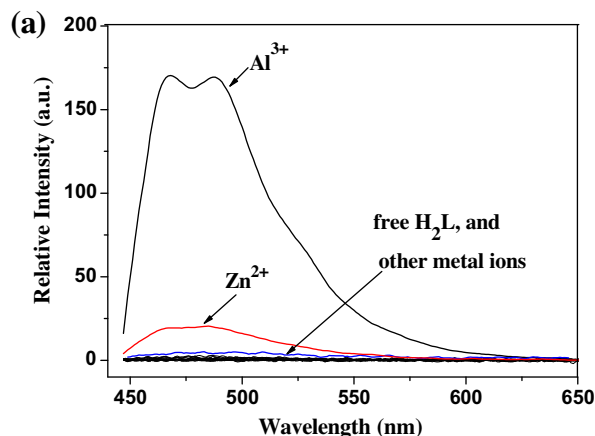


Figure 2. (a) Fluorescence spectra of H₂L (50.0 μM) upon the addition of metal salts (1.0 equiv) of Li⁺, Na⁺, K⁺, Ca²⁺, Mg²⁺, Cu²⁺, Co²⁺, Mn²⁺, Ni²⁺, Zn²⁺, Cd²⁺, Pb²⁺, Fe³⁺, Cr³⁺, and Al³⁺ in DMF. λ_{ex} = 442 nm. (b) A bar graph for fluorescence responses of H₂L (50.0 μM) to various cations (1.0 equiv) in DMF at 466 nm. (c) Fluorescence responses of H₂L (50.0 μM) to various metal ions (1.0 equiv) in DMF at 466 nm. λ_{ex} = 442 nm. The black bars represent the emission intensity of H₂L in the presence of other metal ions. The light gray bars represent emission intensity of a mixture of H₂L with other metal ions followed by addition of Al³⁺ to the solution, respectively.

exhibited three absorption bands at 267, 333, and 380 nm. We further observed changes in the absorbance of H₂L upon addition of Al(NO₃)₃ (Fig. 5a). As there was a gradual addition of Al³⁺ in increasing concentration (0–1.4 equiv), the regular decrease and increase occurred at the bands 380 nm and 435 nm, respectively. A well-defined isosbestic point at ca. 402 nm was observed, indicative of a clean conversion of H₂L into the Al³⁺–H₂L complex. Job's plot (Fig. 5b) which was based on the changes of absorbance at 435 nm, confirmed a 1:1 stoichiometry between Al³⁺ ion and H₂L. Moreover, a positive-ion ESI mass spectrum (Fig. S6), from which we could observe a peak at *m/z* 380.0 assigned to

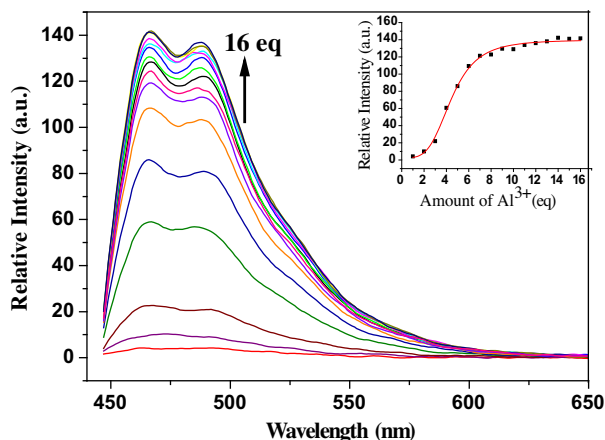


Figure 3. Fluorescence spectra of H₂L (50.0 μM) in DMF upon the addition of Al(NO₃)₃ (0, 1, 2, 3, 4, 5, 6, 7, 8, 9, 10, 11, 12, 13, 14, 15, and 16 equiv) with an excitation of 442 nm. Inset: Fluorescence intensity at 466 nm as a function of the amount of Al³⁺.

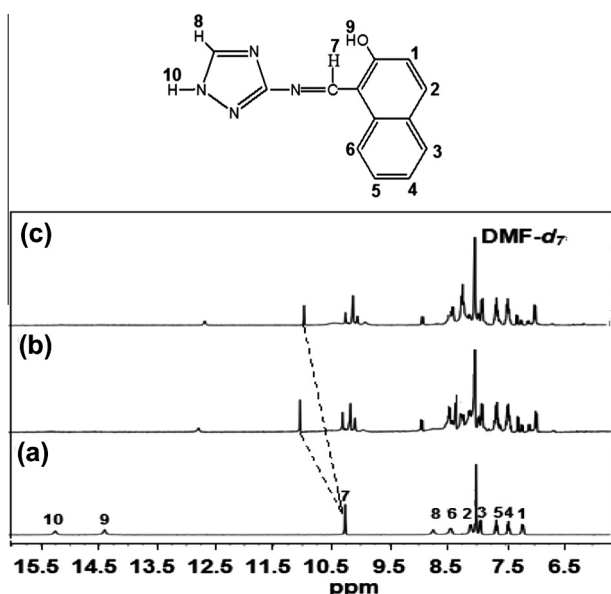


Figure 4. ¹H NMR spectra of H₂L without and with Al(NO₃)₃ in DMF-*d*₇. (a) H₂L only, (b) H₂L and 1.0 equiv of Al³⁺, (c) H₂L and 1.5 equiv of Al³⁺.

[Al(HL)(CH₃CN)₂(H₂O)₂]²⁺ (CH₃CN was solvent), provided additional evidence for the formation of a 1:1 complex of Al³⁺ and H₂L. Furthermore, perfect linear relationships were obtained from the absorption titration profile, from which the association constant (logK_a) of H₂L for Al³⁺ was calculated to be 5.14 and the detection limit was 0.69 μM based on the 3α/slope (Fig. S7). The logK_a of H₂L was within the range of 2.9–14.5 of the reported logK_a for Al³⁺-binding sensors.⁷ The detection limit is lower than the US EPA and FDA guideline of 7.41 μM Al³⁺ for bottled drinking water.¹⁰

Having studied the interesting photophysical properties of H₂L such as high sensitivity and selectivity toward Al³⁺ ions, we further extended our study to evaluating their potential applications in imaging Al³⁺ in cancer cell lines. The confocal fluorescence microscopy measurement was carried out. The human cervical HeLa cancer cells were grown in DMEM (Dulbecco's modified Eagle's medium) supplemented with 10% FBS (fetal bovine serum) at 37 °C and saturated humidity in an incubator in the atmosphere of 5% CO₂ and 99% air. Cells (5 × 10⁸/L) were plated on 14 mm glass cover slips and allowed to adhere for 24 h. After being supplied

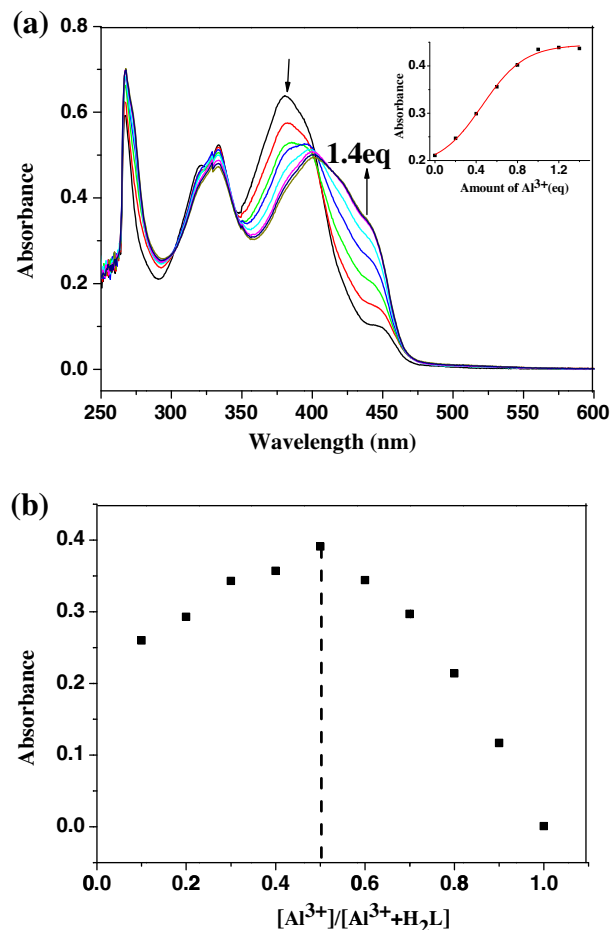


Figure 5. (a) UV-vis spectral changes of H₂L (50.0 μM) in DMF upon the addition of Al(NO₃)₃ (0, 0.2, 0.4, 0.6, 0.8, 1.0, 1.2, 1.4 equiv). Inset: Absorbance at 435 nm was plotted as a function of the amount of Al³⁺. (b) Job's plot for the binding of Al³⁺ with H₂L. Absorbance at 435 nm was plotted as a function of the molar ratio of [Al³⁺]/[Al³⁺+H₂L].

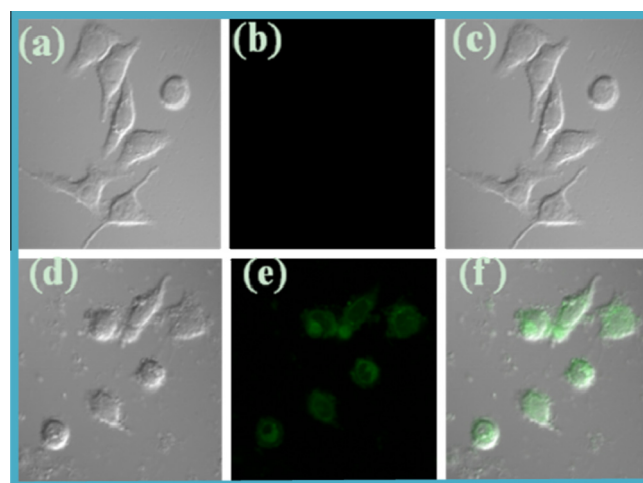


Figure 6. Confocal fluorescence images of Al³⁺ in HeLa cells. Bright-field (a), fluorescent (b) and the overlay (c) images of HeLa cells incubated with Al(NO₃)₃ for 8 h. Bright-field (d), fluorescent (e) and the overlay (f) images of HeLa cells incubated with Al(NO₃)₃ for 8 h and then exposed to 20 μM H₂L for 30 min. λ_{ex} = 405 nm.

mented with 100 μM of Al(NO₃)₃ in the growth media for 8 h at 37 °C, there was no intracellular fluorescence (Fig. 6a–c). After washing with PBS three times to remove any excess Al(NO₃)₃,

the cells were then incubated with 20 μM of H_2L in DMF/PBS (1:99, v:v) solution for 30 min at 37 $^\circ\text{C}$, a significant increase in the fluorescence from the intracellular area was observed (Fig. 6d–f). These results demonstrated that H_2L was membrane permeable and could be used as biosensor to probe the intracellular Al^{3+} .

In summary, we have successfully developed a new Schiff-base fluorescent turn-on chemosensor H_2L which shows high selectivity and sensitivity to Al^{3+} ion in DMF, and displays the 1:1 binding stoichiometry with Al^{3+} . In our assay, Al^{3+} could participate in complex formation with the receptor, which resulted in fluorescence enhancement by CHEF effect. Moreover, the result provides a useful facile strategy for the synthesis and application of a fluorescent sensor to detect intracellular Al^{3+} .

Acknowledgments

This work is supported by the National Natural Science Foundation of China (20971015) and the Fundamental Research Funds for the Central Universities.

Supplementary data

Crystallographic data (excluding structure factors) for the structures in this paper have been deposited with the Cambridge Crystallographic Data Centre as supplementary publication no. CCDC 923333. Copies of the data can be obtained free of charge on application to CCDC, 12 Union Road, Cambridge CB2 1EZ, UK, (fax: +44-(0)1223-336033 or e-mail: deposit@ccdc.cam.ac.uk).

Supplementary data (including synthesis and characterization by elemental analysis, IR and single-crystal X-ray diffraction) associated with this article can be found, in the online version, at <http://dx.doi.org/10.1016/j.tetlet.2013.04.115>.

References and notes

- (a) Robinson, G. H. *Chem. Eng. News* **2003**, *81*, 54; (b) Exley, C. J. *Inorg. Biochem.* **2005**, *99*, 1747–1928.
- (a) Álvarez, E.; Fernández-Marcos, M. L.; Monterroso, C.; Fernández-Sanjurjo, M. J. *Forest Ecol. Manage.* **2005**, *211*, 227–239; (b) Barcelo, J.; Poschenrieder, C. *Environ. Exp. Bot.* **2002**, *48*, 75–92.
- (a) Alstad, N. E. W.; Kjelsberg, B. M.; Vøllestad, L. A.; Lydersen, E.; Poléo, A. B. S. *Environ. Pollut.* **2005**, *133*, 333–342; (b) Delhaize, E.; Ryan, P. R. *Plant Physiol.* **1995**, *107*, 315–321; (c) Ren, J.; Tian, H. *Sensors* **2007**, *7*, 3166–3178.
- (a) Burwen, D. R.; Olsen, S. M.; Bland, L. A.; Arduino, M. J.; Reid, M. H.; Jarvis, W. R. *Kidney Int.* **1995**, *48*, 469–474; (b) Fasman, G. D. *Coord. Chem. Rev.* **1996**, *149*, 125–165; (c) Nayak, P. *Environ. Res.* **2002**, *89*, 101–115; (d) Cronan, C. S.; Walker, W. J.; Bloom, P. R. *Nature* **1986**, *324*, 140–143; (e) Berthon, G. *Coord. Chem. Rev.* **2002**, *228*, 319–341; (f) Martin, R. B. *Acc. Chem. Res.* **1994**, *27*, 204–210; (g) Bielarczyk, H.; Jankowska, A.; Madziar, B.; Matecki, A.; Michno, A.; Szutowicz, A. *Neurochem. Int.* **2003**, *42*, 323–331; Yousef, M. I.; El-Morsy, A. M.; Hassan, M. S. *Toxicology* **2005**, *215*, 97–107.
- (a) Alfrey, A. C. *Adv. Clin. Chem.* **1983**, *23*, 69–91; (b) Perl, D. P.; Gajdusek, D. C.; Garruto, R. M.; Yanagihara, R. T.; Gibbs, C. J. *Science* **1982**, *217*, 1053–1055; (c) Perl, D. P.; Brody, A. R. *Science* **1980**, *208*, 297–299.
- (a) Maity, D.; Govindaraju, T. *Inorg. Chem.* **2010**, *49*, 7229–7231; (b) Kim, S. H.; Kim, J. S. *Org. Lett.* **2010**, *12*, 560–563; (c) Maity, D.; Govindaraju, T. *Chem. Commun.* **2010**, *46*, 4499–4501; (d) Ma, T. H.; Wang, Y.-W.; Peng, Y. *Chem. Eur. J.* **2010**, *16*, 10313–10318; (e) Kim, J. S.; Vicens, J. *Chem. Commun.* **2009**, *45*, 4791–4802; (f) Wang, Y.-W.; Shen, Z.; Li, F.-Y. *Tetrahedron Lett.* **2009**, *50*, 6169–6172; (g) Lin, W. Y.; Yuan, L.; Feng, J. B. *Eur. J. Org. Chem.* **2008**, 3821–3825; (h) Jung, J.-Y.; Han, S.-J.; Chun, J.; Lee, C.; Yoon, J. *Dyes Pigment.* **2012**, *94*, 423–426; (i) Hau, F. K.-W.; He, X.; Lam, W. H.; Yam, V. W.-W. *Chem. Commun.* **2011**, *47*, 8778–8780; (j) Lu, Y.; Huang, S.; Liu, Y.; He, S.; Zhao, L.; Zeng, X. *Org. Lett.* **2011**, *13*, 5274–5277; (k) Kim, S.; Noh, J. Y.; Kim, K. Y.; Kim, J. H.; Kang, H. K.; Nam, S. W.; Kim, S. H.; Park, S.; Kim, C.; Kim, J. J. *Inorg. Chem.* **2012**, *51*, 3597–3602.
- (a) Arduini, M.; Felluga, F.; Mancin, F.; Rossi, P.; Tecilla, P.; Tonellato, U.; Valentinuzzi, N. *Chem. Commun.* **2003**, 1606–1607; (b) Lohani, C. R.; Kim, J. M.; Chung, S.-Y.; Yoon, J.; Lee, K.-H. *Analyst* **2010**, *135*, 2079–2084; (c) Jang, H. O.; Nakamura, K.; Yi, S.-S.; Kim, J. S.; Go, J. R.; Yoon, J. J. *Inclusion Phenom. Macrocycl. Chem.* **2001**, *40*, 313–316; (d) Ren, J.-L.; Zhang, J.; Luo, J.-Q.; Pei, X.-K.; Jiang, Z.-X. *Analyst* **2001**, *126*, 698–702; (e) Wang, Y.-W.; Yu, M.-X.; Yu, Y.-H.; Bai, Z.-P.; Shen, Z.; Li, F.-Y.; You, X.-Z. *Tetrahedron Lett.* **2009**, *50*, 6169–6172; (f) Kim, S. H.; Choi, H. S.; Kim, J.; Lee, S. J.; Quang, D. T.; Kim, J. S. *Org. Lett.* **2010**, *12*, 560–563; (g) Maity, D.; Govindaraju, T. *Eur. J. Inorg. Chem.* **2011**, *50*, 5479–5485; (h) Sun, X.; Wang, Y. W.; Peng, Y. *Org. Lett.* **2012**, *14*, 3420–3423.
- (a) Lou, X. D.; Ou, D. X.; Li, Q. Q.; Li, Z. *Chem. Commun.* **2012**, *48*, 8462–8477; (b) Ngo, H. T.; Liu, X. J.; Jolliffe, K. A. *Chem. Soc. Rev.* **2012**, *41*, 4928–4965; (c) Shellaiah, M.; Wu, Y. H.; Singh, A.; Raju, M. V. R.; Lin, S. C. J. *Mater. Chem. A* **2013**, *1*, 1310–1318; (d) He, G. J.; Zha, Y. G.; He, C.; Liu, Y.; Duan, C. Y. *Inorg. Chem.* **2008**, *47*, 5169–5176; (e) Brenlla, A.; Veiga, M.; Lustres, J. L. P.; Rodriguez, M. C. R.; Rodriguez-Prieto, F.; Mosquera, M. J. *Phys. Chem. B* **2013**, *117*, 884–896.
- (a) Dong, Y.; Li, J.; Jiang, X.; Song, F.; Cheng, Y.; Zhu, C. *Org. Lett.* **2011**, *13*, 2252–2255; (b) Park, H. M.; Oh, B. N.; Kim, J. H.; Qiong, W.; Hwang, I. H.; Jung, K.-D.; Kim, C.; Kim, J. *Tetrahedron Lett.* **2011**, *52*, 5581–5584.
- Sun, X.; Wang, Y.-W.; Peng, Y. *Org. Lett.* **2012**, *14*, 3420–3423.